JOURNAL OF MATERIALS SCIENCE **39** (2004) 3889– 3899

Influence of residual stresses in the performance of cold-drawn pearlitic wires*

M. ELICES
Departamento de Ciencia de Materiales, Universidad Politécnica de Madrid, E.T.S. Caminos, Profesor Aranguren s/n, 28040—Madrid, Spain
E-mail: melices@mater.upm.es

The mechanical properties of cold-drawn pearlitic wires are controlled largely by the microstructure developed during processing and, to some extent, by the residual stresses during drawing. The advent of powerful computers and the availability of equipment to perform diffraction experiments, have made possible numerical predictions and accurate measurements of residual stresses. This paper—a review of work done by the author and collaborators—shows how *stress-relaxation losses*, *environmental assisted cracking* and *fatigue life* of cold-drawn pearlitic wires are influenced by residual stresses. The role of pre-stretching loads, or of stress relieving treatments, on stress-relaxation can be understood when the profile of residual stresses is known. Some awkward results in times to fracture during hydrogen embrittlement tests can be explained if accurate values of residual stresses near the surface are known, and the same is true of fatigue life. In this context *numerical simulations* and *measurements* performed on cold-drawn pearlitic wires, with different profiles of residual stresses, have shown very good quantitative agreement.

1. Cold drawn pearlitic wires: Strength and toughness

The highest tensile strength in metallic wires is exhibited by cold-drawn pearlitic wires, in which values of 5700 MPa have been reported for very thin wires of 0.04 mm diameter [1]. Pearlitic cold-drawn wires and strands are the active tendons in prestressed concrete structures, support the tensile stresses in suspension and modern stayed bridges, and form the cables in deeper mine shafts and off-shore petroleum production. They are also a main ingredient in the tyre industry, as reinforcing steel cords. Production of steel cord wire alone is about 1 million tons per year and the world estimated production of pearlitic drawn wire is above 25 million tons per year [2].

Eutectoid cold-drawn pearlitic wire is —in present day terminology— a nano.composite, nano.laminate and nano.prestretched material, with outstanding properties of strength and toughness that are still amazing to the modern metallurgist and materials engineer. The origins of metallic wires are well rooted in time. It is documented that wire was in use before 3.000 B.C., probably made by hammering and folding softer metals. The drawing process was mentioned in the writings of the Roman tribune Claudius Claudianus in 400 A.D. Wire drawers flourished in the Middle Ages and the drawing industry was recognized as a trade and proceeded slowly until the end of the XIX century. As mentioned by A.B. Dove [3]: "It speaks well for the versatility of the wire drawer that he was able by rule of thumb methods to draw a good high grade wire of reasonably consistent quality." The advent of continuous drawing machines and hard materials for drawing dies —such as widia— brought the development of the drawn wire industry of the XX century.

The mechanical behaviour of cold-drawn pearlitic wires, particularly their tensile strength and toughness, is controlled largely by the microstructure developed during processing. Fig. 1 displays the increase in strength as microstructure was improved, of wires for reinforcing tyres and of cables for suspension bridges.

In the drawing of wire, the *tensile strength* of pearlite increases, roughly, as the exponential of drawing strain. At high strains, the reorientation of lamella and the development of fine dislocation cells are also important sources of strengthening [4]. The yield strength may be considered as the sum of the strengthening effects from various mechanisms [5]: Strengthening from *interlamellar spacing refinement*; interlamellar spacing of tens of nanometers is achieved during wire drawing (Fig. 2). Alloy strengthening, due to *solid-solution strengthening* and *composite strengthening*, increases as the volume fraction of cementite in pearlite increases. Strengthening from the *pearlite colony size* should

*This paper is dedicated to Professor Robert W. Cahn. Cold-drawn eutectoid steel wire is a noble material with a long tradition and rich in possibilities of new disclosures. The same may be said of Professor Cahn; the better we know him the more stimulating he appears. I wish him a long period of activity as he still has a great deal up his sleeve.

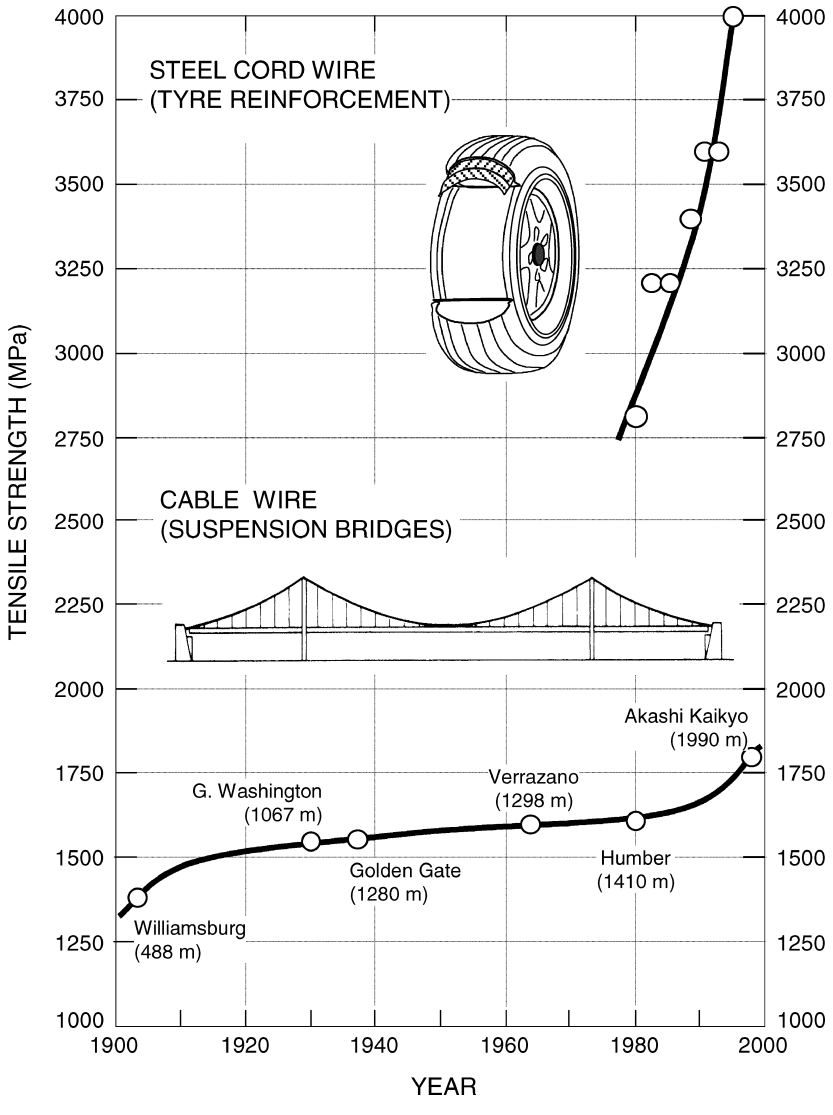

Figure 1 Historical development of the tensile strength of cold-drawn steel wires. The lower curve corresponds to steel wires for bridge cables. The suspension bridge spans (in meters) are also shown. The upper figure is for steel cord wire for tyre reinforcement (based on [6, 7]).

also be considered. Another significant component of strengthening is that of *fine dislocation cells* that develop in the ferrite lamina of heavily deformed pearlite.

The *fracture toughness* of cold drawn steel wires is more difficult to measure on account of the marked degree of fracture anisotropy which results from the drawing process. It is much easier to propagate cracks in the longitudinal than in the transverse direction. This behaviour favours stress release at the tip of small cracks to the extent of stopping incipient stress corrosion cracks [8]. A review of fracture and fracture toughness measurements of steels for reinforcing and prestressing concrete, published in 1984, is still of value [9], and limited data on the fracture toughness of drawn eutectoid and hypereutectoid steel wires have been reported since then. Fig. 3 shows fracture toughness values, at different temperatures, for longitudinal and transverse cracked specimens of cold drawn eutectoid steel wires, 7 mm diameter and 0.2% proof stress $\sigma_{0.2} = 1590$ MPa. Longitudinal values are most probably valid up to -60°C due to plasticity. Transverse values at low and room temperatures are suspicious because the crack tends to leave the transverse plane and propagate in a longitudinal direction. More recent results on cold-drawn wires of small diameter, 1.84 mm and $\sigma_{0.2} = 1517$, 1620 and 1792 MPa provided values, at room temperature, of 59, 65 and 64 MPa $\sqrt{\text{m}}$ [10]. Early attempts to measure the fracture toughness and to characterize the anisotropic fracture behaviour of cold-drawn steels are found in [9, 11, 12].

This paper summarizes the work done by the author and collaborators during the last years, attempting to correlate quantitatively the presence of the residual stresses induced during wire drawing with the tensile properties, particularly, with *stress relaxation losses* over time or with subcritical crack propagation in *fatigue life* or *environmental assisted cracking*. In all cases, very good agreement was found between experimental measurements and numerical simulations.

2. Residual stresses due to cold drawing: Computation and measurement

Steel wires suffer a large plastic deformation during the drawing process. After drawing, strains tend to recover but if hampered somewhere by previous plastic deformation, a field of residual strains—and hence, stresses—may appear.

Figure 2 AFM picture of the pearlitic microstructure of a eutectoid steel, patented and cold-drawn. The sample was etched; valleys were filled with ferrite, and the ridges are of cementite, in some places plastically deformed. The height of the ridges is about 200 nm (courtesy of B. Monteiro).

Very briefly, cold drawing consist of pulling a lubricated bar through a die (Fig. 4), thus reducing its cross-sectional area and increasing its length. The speed of drawing is highly dependent on the class of planned wire and can vary from tenths of a meter to several meters per second. Commercial wire-drawing machines use several dies in series (Fig. 4). The number and the type of dies depend upon the finishing size of wire and on the intended product. After drawing, it may be advisable to perform some thermo-mechanical treatments to modify the residual stresses or to obtain specific properties in the finished wire.

Residual stresses can be *computed* numerically. We simulated the drawing process using the finite element method [13] with the help of ABAQUS Code [14]. A three-dimensional Lagrangian formulation was used for the wire, which was modelled as an elastoplastic material with strain hardening. Isotropic hardening with a von Mises criterion was considered and, as a first approximation, the yield locus was assumed independent of strain rate. Special care was taken in choosing the finite elements to avoid the well known volumetric locking problem [13, 15, 16]. The initial stress-strain function of the wire elements was that obtained experimentally from a tensile test performed with a sample of the wire, before being drawn. The die was also modelled using the finite element method and the material was assumed linear elastic with a modulus of elasticity

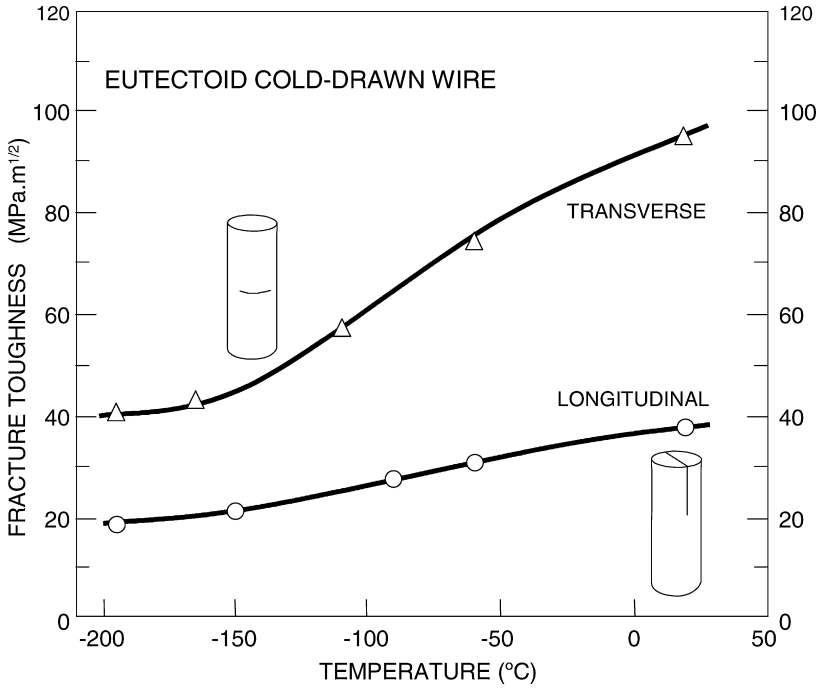

Figure 3 Fracture toughness of eutectoid cold-drawn steel wires (7 mm diameter) at different temperatures [9].

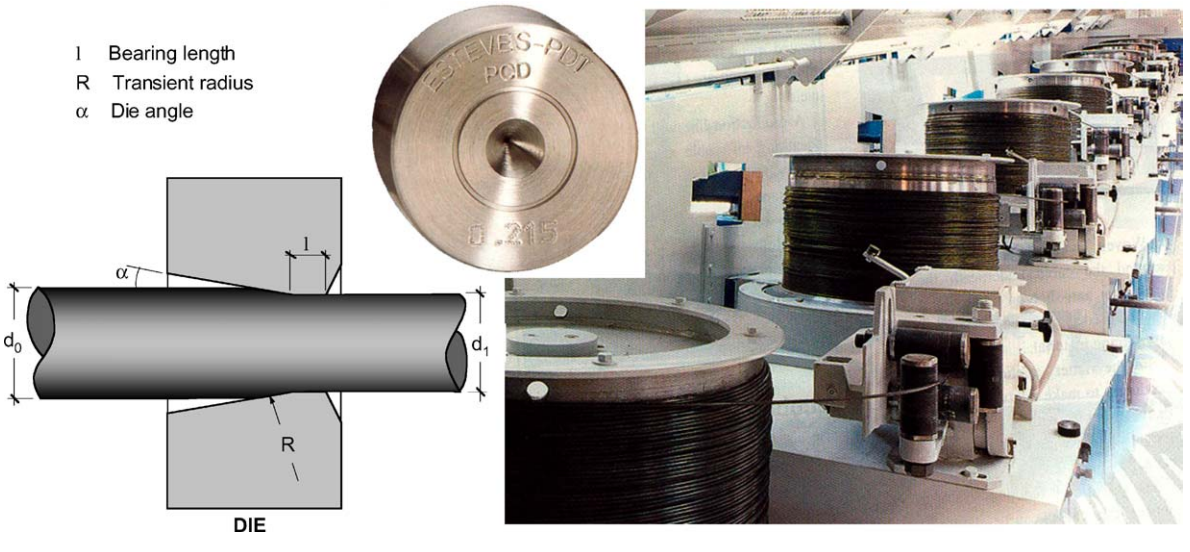

Figure 4 (Left) Die geometry used for cold-drawing. (Right) View of commercial wire-drawing machines. (Insert, a picture of a die).

of 600 GPa, similar to widia. The contact between wire and die was modelled as Coulomb friction, with a friction coefficient ranging between 0.2 and 0.01 [17]. A detailed description of the numerical modelling is given in [18]. It was found that cold-drawing generates an axisymmetrical profile of residual stresses, due to an inhomogeneous plastic deformation through the die. As an example, Fig. 5 shows a profile of computed longitudinal residual stresses, as a function of relative depth, after eight drawing passes, of a eutectoid pearlitic steel wire of initial diameter of 12 mm and a final one of 5.2 mm. The final mechanical properties of cold-drawn wire were: $\sigma_{0.2} = 1720$ MPa, $\sigma_{\max} = 1940$ MPa and elongation under maximum load, $\varepsilon_{\mathrm{m}} = 1.9\%$.

Residual stresses can also be *measured* (see, for example [19]). In polycrystalline materials, the elastic strain of the crystal lattice —caused by the internal stress— is measured by measuring the spacing of some lattice plane and comparing it to the lattice spacing of a stress-free material. Lattice spacing is measured from the diffraction pattern of a beam of waves. Beams of X-ray, or neutrons, are used for this purpose. The average macroscopic residual stresses in pearlitic eutectoid steels —a two-phase lamellar mixture of ferrite and cementite— are difficult to evaluate because diffraction techniques provide separate values of the ferrite and cementite phases. Moreover, the diffraction peaks of the cementite are very weak and hard to interpret. In addition, severe plastic deformation, due to cold-drawing, increases the difficulties.

Reliability on computed residual stresses is based on previous experience with drawn ferritic and pearlitic wires:

(a) First, a previous research on cold drawn ferritic wires, summarized in [20], served to calibrate and tune

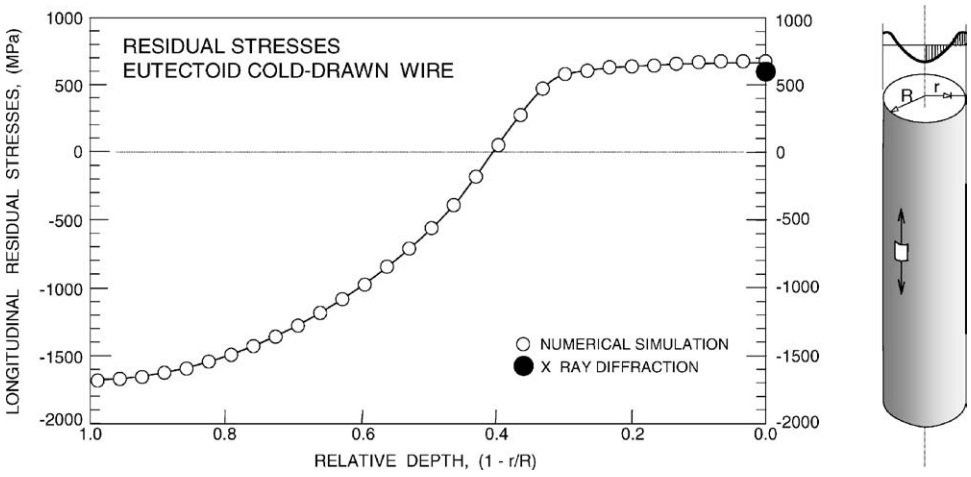

Figure 5 Computed longitudinal residual stresses in drawn eutectoid steel wires (positive values correspond to tensile stresses). Also shown, surface residual stresses based on X-ray diffraction measurements of the ferrite phase.

the experimental and numerical techniques. Stresses in single phase ferritic cold-drawn bars were numerically computed and also measured by neutron and X-ray diffraction. Neutron measurements were performed in a reactor based source at NFL-Studsvik, Sweden, with the REST diffractometer, a two-axis high resolution device equipped with a double focussing monochromator that provides a neutron beam of wave length between 0.166 and 0.176 nm. A position-sensitive detector was used. X-ray measurements were performed with a Rigaku Strainflex analyser with Cr K_α radiation, (wave length 0.229 nm). The diffractometer was used in Ω-mode with the $\sin^2\psi$ method. For details of these diffraction techniques see ref. [21]. Computed and experimental measurements of longitudinal stresses, at different depths, in the cold-drawn bar are given in Fig. 6. The stress profile is in self-equilibrium and high tensile residual stresses —around 250 MPa— appeared on the wire surface. The agreement between numerical and experimental values was excellent.

(b) The next step was to repeat the previous research with a cold-drawn pearlite wire —a two phase material—. The numerical simulation did not pose new problems. From the experimental side, however, the weak signal from the cementite phase, as already mentioned, was the main difficulty we found. Work is in progress to match experimental and numerical results. Recent findings suggest that the cementite phase on the wire surface may withstand tensile stresses of about 2500 MPa [22]. From this value and the measured values of the ferrite phase, and using the simple rule of mixtures, average experimental values can be computed on the surface. It happens that these values coincide quite well with numerical predictions, as shown in Fig. 5. These results give additional support to the numerical computations.

3. Residual stresses and the tensile test

3.1. Setting the stage

It is known that the presence of residual stresses can alter the shape of the stress-strain curve of a tensile test, particularly the onset of yielding and the nearby region, usually known as the preplastic region. Standards for cold-drawn wires for prestressing concrete [23] require minimum and maximum figures for $\sigma_{0.2}/\sigma_{max}$, as

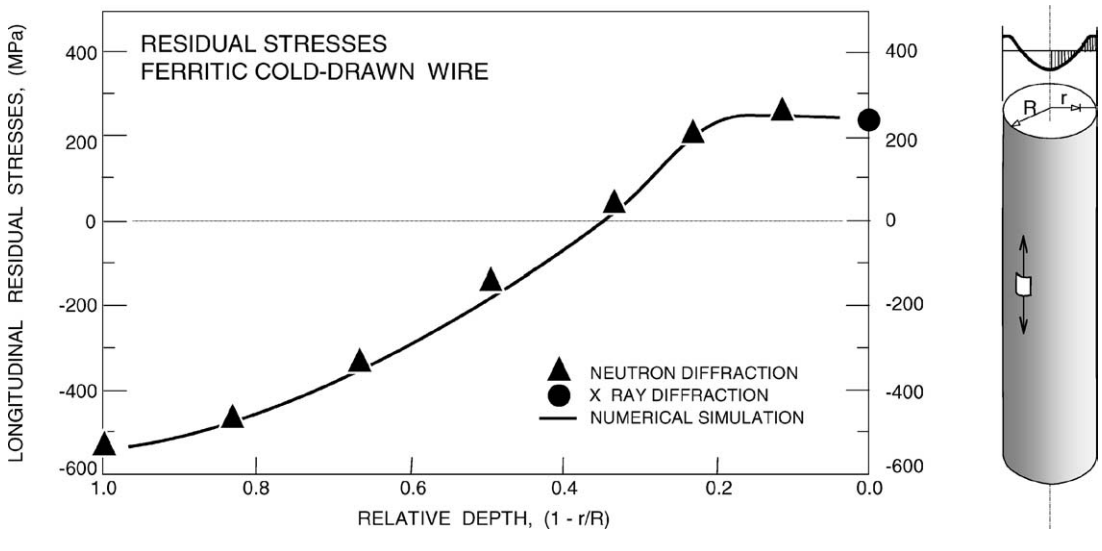

Figure 6 Measured (by neutron and X-ray diffraction) and computed residual stresses in drawn ferritic steel wires (positive values correspond to tensile stresses).

TABLE I Average tensile values of eutectoid bars

	$\sigma_{0.2}$(MPa)	σ_{max} (MPa)	$\varepsilon_{\sigma\,(max)}$
Before drawing	515	945	8.6
After drawing	940	1115	2.2
Additional 1% reduction	1065	1131	1.7
Thermomechanical treatment	1135	1200	1.9

measured in a tensile test. The rationale behind these figures seems to be based on good practice and on the idealized behaviour of a prestressing tendon [3, 24] and, to the author's knowledge, the role of residual stresses in shaping this region —and hence its beneficial or damaging influence— had not been quantified. To explore this behaviour, an experimental program and a numerical simulation of the processes were set up. Some of these results, published in [25], are summarized below.

3.2. Experimental and numerical results

Eutectoid steel bars, 20 mm diameter, were used for this task. The bars were cold-drawn to 18 mm diameter (20% reduction of area). Table I summarizes the average tensile values of tensile tests for bars before and after drawing.

Residual stresses due to cold-drawing are known to be detrimental to the mechanical performance —particularly as regards creep, fatigue and ductility— and different procedures were devised to eliminate or decrease such stresses. Two procedures were considered here: One was a further drawing with a very small area reduction (about 1%), and another was based on a combination of heating and stretching the wire. (Heating at 400°C under a tensile load of $0.4\sigma_{max}$).

The experimental work, in short, was: drawing the bars, performing the two mentioned treatments, and finally performing tensile tests. Longitudinal surface stresses were also measured in the ferrite phase using X-ray diffraction. The average macro stress in the pearlite surface was computed as previously mentioned in 2.

The numerical approach consisted in simulating the drawing process (the stress-strain curve of the bar before drawing was used as the input data) and the tensile test after drawing. A second drawing pass, with 1% reduction of area, was also simulated as well as the corresponding tensile test. Finally, the thermomechanical treatment and its corresponding tensile test were also computed.

Fig. 7a shows the corresponding profiles of longitudinal residual stress as a function of relative depth. Surface values, computed from X-ray diffraction measurements of the ferrite phase, are also shown. The post drawing treatments are seen to decrease substantially the residual stresses. Fig. 7b shows the stress-strain curves of wires as drawn, with the additional (1%) drawing, and with the thermomechanical treatment. Characteristic values are also given in Table I. Experimental and numerical results for these three curves are indistinguishable, which gives additional support to the numerical approach.

3.3. Conclusions

From this research it was found that the presence of residual stresses due to standard cold-drawing (tensile stresses on the surface) favours the onset of yielding (see Fig. 7). The higher the residual stresses the lower is the yield stress in a tensile test.

From the average values quoted in Table I, one can conclude that the ratio $\sigma_{0.2}/\sigma_{max}$ decreases with increasing values of residual stresses. Because of the deleterious effect of tensile surface residual stresses on fatigue, stress-corrosion and stress-relaxation, it is reasonable to put a lower limit to $\sigma_{0.2}/\sigma_{max}$. The ratio $\sigma_{0.2}/\sigma_{max}$ can be increased by relieving residual stresses, a common procedure after drawing. These techniques may help in placing the ratio $\sigma_{0.2}/\sigma_{max}$ within the figures recommended in the standards.

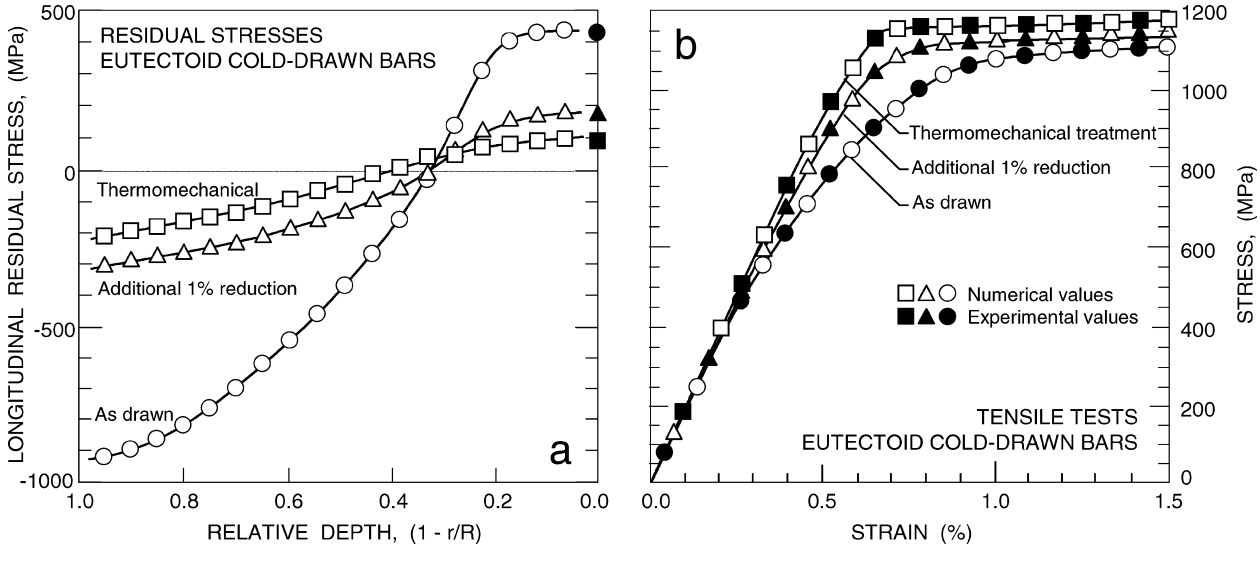

Figure 7 (a) Profiles of computed longitudinal residual stresses. Surface values, computed from measurements of the ferrite phase are also shown. (b) Stress-strain curves —measured and computed— for drawn wires, with additional (1%) drawing and with a thermomechanical treatment.

4. Time and residual stresses

4.1. Setting the stage

Creep is the change in strain, with time, in a material held under constant stress, whereas *stress relaxation* is the loss of stress in a material held at a constant strain. In cold-drawn wires, both aspects of this viscoplastic phenomenon are influenced by the presence of residual stresses.

In prestressed concrete structures, stress relaxation losses in steel wires are of paramount importance and design codes place limits on initial stretching loads as well as recommendations for keeping the relaxation losses within safe margins. The role, sometimes controversial, of pre-stretching loads on stress relaxation losses can be partially understood in the light of the residual stresses induced during cold-drawing.

The influence of residual stresses (due to cold drawing) on the stress relaxation of steel wires was ascentained in a previous study [20] and some of these results, together with research in progress, are summarized here.

4.2. Experimental and numerical results

In the first part of this research, ferritic bars were chosen because in this single-phase material residual stresses can be measured by X-ray diffraction with high accuracy. As it was intended to measure the stress distribution across the wire section by neutron diffraction, bars of 20 mm diameter were selected. This large size allowed measurements at thirteen points across the diameter. The bars were cold-drawn, in one pass, to a final diameter of 18 mm (20% reduction in section). The main average parameters obtained from tensile tests are summarized in Table II.

To compare the relaxation behaviour of steel wires with different residual stresses it was necessary to have samples with the same σ_{max} and different profiles of residual stresses, as the standardized relaxation test [26] requires an initial load of 0.70 of the ultimate tensile load. Pre-stretching the wires at stresses below the yield stress has proven an easy way to modify the residual stress profile without changing significantly the ultimate tensile load. Two sets of bars were prepared by pre-stretching the drawn bar at $0.70\sigma_{0.2}$ and at $0.82\sigma_{0.2}$. The average values of σ_{max} after pre-stretching are shown in Table II and are seen to be similar to the corresponding value of the drawn bar.

TABLE II Average tensile values of ferritic bars

	$\sigma_{0.2}$ (MPa)	σ_{max} (MPa)	$\varepsilon_{\sigma\,(max)}$
Before drawing	230	340	2.2
After drawing	475	500	1.6
Pre-stretched 0.70 $\sigma_{0.2}$	477	502	1.6
Pre-stretched 0.82 $\sigma_{0.2}$	482	500	1.6

Stresses in cold-drawn bars were measured by neutron and X-ray difraction. Fig. 8a shows longitudinal residual stresses as a function of relative depth. Details of these measurements were published elsewhere [20, 21]. After pre-stretching, residual stresses were also measured by X-ray diffraction on the surface of the bars. The experimental values are also shown in Fig. 8a.

At the same time, a numerical simulation of the drawing process was performed by the procedures already mentioned (a detailed description was given in refs. [18, 20]), and residual stresses were computed at the end of the drawing process. Values of the longitudinal stresses, at different depths, are shown in Fig. 8a. The pre-stretching treatments were also simulated numerically and the final profiles of residual stresses are also given in Fig. 8a. The agreement between numerical and experimental values for drawn bars is very good, and the same applies to the surface values of pre-stretched bars.

Finally, stress relaxation losses were measured —according to [26]— in the three types of bars —all with the same σ_{max} and different profiles of residual stresses—. The results are shown in Fig. 8b.

The second part of this research with eutectoid cold-drawn wires is under way. Stress relaxation tests were

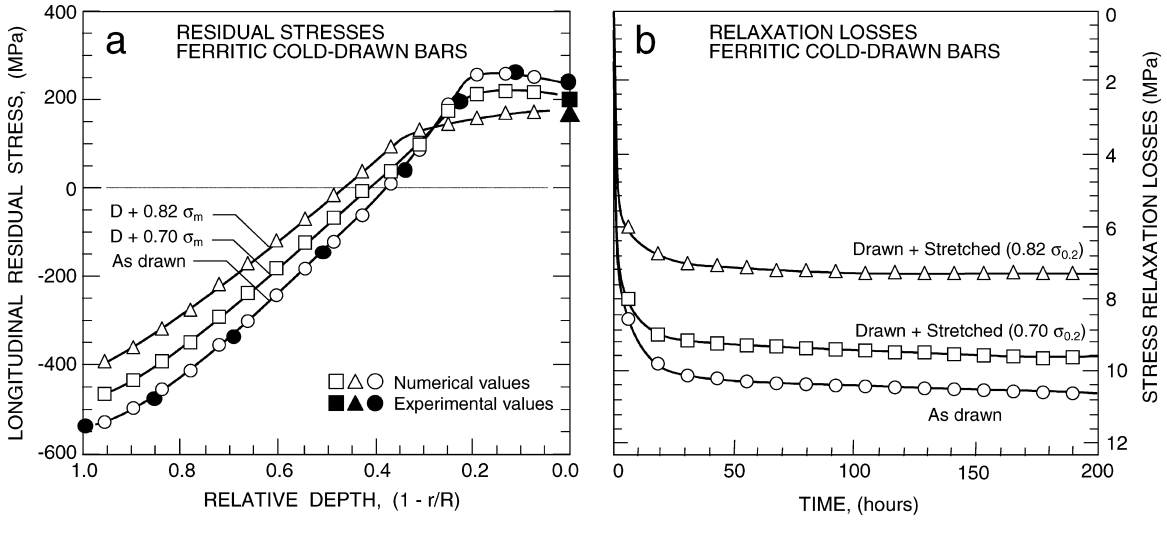

Figure 8 (a) Profiles of computed (open symbols) and measured (full symbols) residual stresses in ferritic bars, as a function of relative depth. (b) Measured stress relaxation losses in ferritic bars with the same ultimate tensile load and different residual stresses.

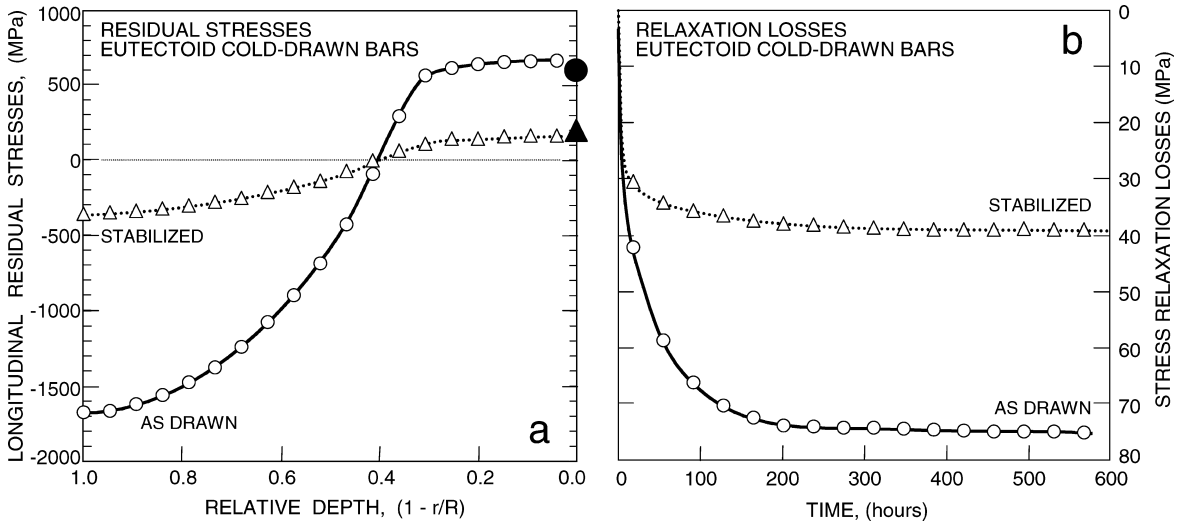

Figure 9 (a) Profiles of computed (open symbols) residual stresses in eutectoid wires as a function of relative depth. Surface values, from measurements of the ferrite phase, are also shown (full symbols). (b) Measured stress relaxation losses in eutectoid wires [27].

performed with eutectoid steel wires, 5.2 mm diameter, [27]. Here, one wire was as drawn (with high residual stresses) and another was stabilized by a commercial procedure to lower residual stresses. Computed profiles of longitudinal stresses and measured values at the surface by X-ray diffraction (on the ferrite phase, as already explained) are shown in Fig. 9a. Measured stress losses after 600 h, for both steels, are also shown in Fig. 9b.

4.3. Conclusions

The experimental results show a clear relationship between stress relaxation and the presence of residual stresses; stress relaxation losses increase with the increase of surface tensile residual stresses (see Figs 8b and 9b).

Cold-drawn wires with the same mechanical properties required by standards (i.e., with the same yield stress, ultimate tensile stress, and elongation under maximum load) but with different residual stresses will exhibit different stress relaxation behaviour. To correlate the mechanical behaviour of cold-drawn wires and the role of pre-stretching loads with stress relaxation losses, it is necessary to take into account the residual stresses induced during cold-drawing and modified by further treatments.

5. Subcritical crack propagation and residual stresses

Delayed fracture of cold-drawn eutectoid steel wires, a worrying problem not yet satisfactorily solved, may be due to subcritical crack propagation as in failures due to fatigue, or to environmental assisted cracking —as in stress corrosion or hydrogen embrittlement fracture—, or to a combination of both. In either circumstance, residual stresses play an important role. A brief review of work done by the author and collaborators in this area is summarized in the two following paragraphs.

5.1. Influence of residual stresses on fatigue life

The development of a dominant crack from the wire surface under high cycle fatigue occupies the major part of the fatigue lifetime [28]. Therefore, an accurate calculation of the fatigue life requires an accurate knowledge of the surface stresses, which are dependent on the external loads and on residual stresses.

An experimental and numerical investigation of the influence of residual stresses in cold-drawn eutectoid steels —particularly on the fatigue limit and on the fatigue life— was undertaken some years ago. Results were reported in [29, 30] and some conclusions are summarized here.

Eutectoid steel rods, 12 mm diameter, were cold-drawn to 7 mm diameter wires in six passes. The drawn wires were stress relieved by heating at about 450°C for a few seconds. The average mechanical properties were: $\sigma_{0.2} = 1370$ MPa, $\sigma_{\max} = 1720$ MPa and $\varepsilon_{\sigma(\max)} = 5.0\%$. Before fatigue testing, surface residual stresses were measured by X-ray diffraction. High scatter was found and tensile values below 100 MPa were measured. Several specimens were fully rolled at different pressures to modify surface and sub-surface residual stresses. Measurements of surface stresses on rolled samples gave compressive stresses of between 200 and 400 MPa. Fatigue tests were performed at a constant stress range and at different nominal stress ratios ($R = \sigma_{\min}/\sigma_{\max}$). Fatigue tests were also modelled, as described in [30].

Agreement between experimental and numerical results for fatigue life and fatigue thresholds was very good. The fatigue life in the high stress ranges showed little influence of residual stresses. In ranges close to the threshold, the fatigue life displayed a strong dependence on the residual stresses and the shape of initial flows. The influence of residual stresses on the fatigue threshold was important at small stress ratios. Recent work, done by other authors [31] with cold-drawn eutectoid steel wires of 0.3 mm diameter, showed similar results, i.e., that the residual stress is one of the controlling factors of the fatigue threshold.

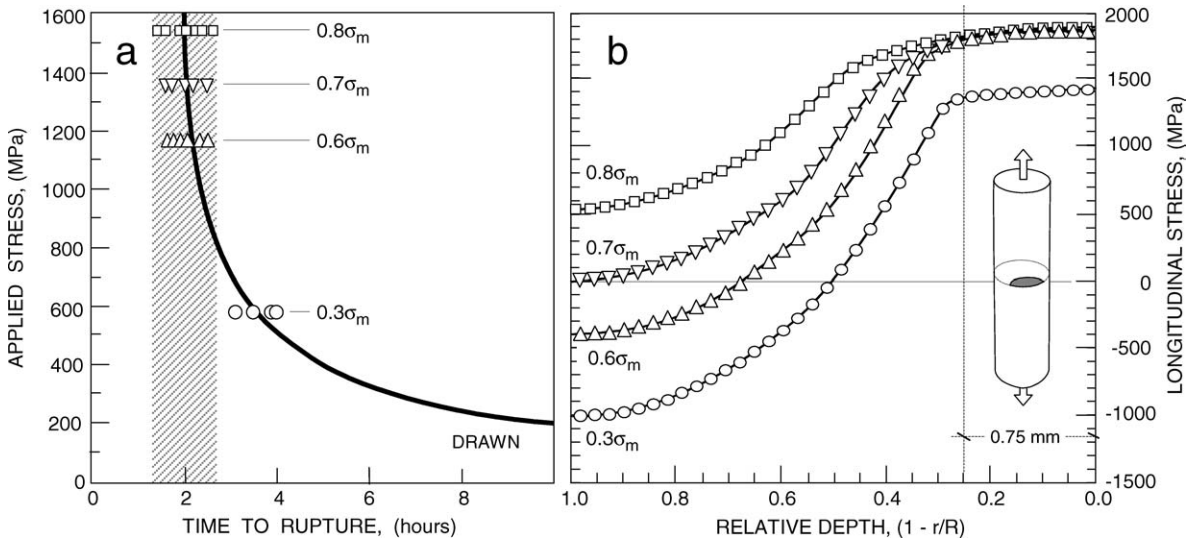

Figure 10 Wires with high tensile surface residual stresses showed similar times to rupture when loaded above certain values: (a) Hydrogen embrittlement test. Rupture times for eutectoid cold-drawn wires. (b) Profiles of longitudinal stresses when the wire is stressed at different loads as a function of the relative depth ($\sigma_m = 1940$ MPa).

5.2. Influence of residual stresses on environmental assisted cracking

Experience has shown that cracks in cold-drawn eutectoid wires can grow at stress intensities well below the fracture toughness of the material, under the combined action of stress and an aggressive environment. This phenomenon —known as *environmental assisted cracking*— is one of the problems of concern in steels for prestressing concrete, although it is well known that when these steels are protected by sound and uncracked concrete their durability is guaranteed.

There is general agreement that hydrogen embrittlement plays an important role in the environmental cracking of eutectoid cold-drawn steels [32]. To control the susceptibility of these steels to hydrogen embrittlement, a simple test —based on a solution of ammonium thiocyanate— was proposed by the International Federation of Prestressed concrete FIP [33]. This test is suitable for quality control of one grade of steel and for comparison of different grades of the same type of steel. The FIP test, in addition to its specificity, has the drawback of the scatter in the rupture time. This time is influenced by surface defects and by the presence of residual stresses, as was shown some time ago by the author and collaborators [34, 35]. Improvements, since then, in the measurement of residual stresses and in computing power has provided more information on this subject. Recent work on the role of residual stresses in the hydrogen embrittlement of eutectoid cold-drawn wires, [36], is summarized as follows.

Two batches of eutectoid steel wires, 5.2 mm diameter, for prestressing concrete —with different residual stresses— were tested according to FIP recommendations. The steels selected for this research had the same microstructure and similar mechanical properties, as shown in Table III.

Macroscopic residual stresses in cold-drawn eutectoid wires were computed, and longitudinal surface stresses measured by X-ray diffraction were obtained by the procedures already mentioned. Profiles of longitudinal stresses, as a function of relative depth, are shown in Fig. 9a.

Good correlation was found between times to rupture in the FIP test and residual longitudinal stresses: Drawn wires, with high tensile surface residual stresses —about 600 MPa— showed an average time to rupture of 2.0 h. Stabilized wires, with lower tensile residual stresses —about 200 MPa— lasted, on average, 4.2 h.

The presence of residual stresses also elucidated some puzzling experimental results: Wires with high tensile surface residual stresses showed similar times to rupture when loaded above certain values (for example, at 0.8, 0.7 or 0.6 of the tensile strength). This experimental result can be explained if the combined action of external loads and residual stresses surpasses the yield stress in the outer layers of the steel wire; additional loads or higher residual stresses hardly increase the stresses on the wire skin where crack initiation is suspected to arise [34, 35]. Fig. 10 exemplifies this fact when wires are loaded (in the hydrogen embrittlement test) at $0.8\sigma_{max}$, $0.7\sigma_{max}$ or $0.6\sigma_{max}$; the stresses near the wire surface (to a depth of 0.75 mm) are the same, and it is in this region that cracks develop and grow to the critical size. Any defect inside this region, able to trigger the brittle fracture, will behave in the same way, and times to rupture should be the same. Another interesting result is shown in Fig. 11. Wires with the same microstructure, surface quality and mechanical properties may show similar times to fracture when tested at quite different loads; drawn wires, tested at very low loads ($0.3\sigma_m$) show similar times to rupture as stabilized wires tested at high loads ($0.8\sigma_m$). Again, the profile of

TABLE III Average tensile values of cold-drawn eutectoid wires

	$\sigma_{0.2}$ (MPa)	σ_{max} (MPa)	$\varepsilon_{\sigma\,(max)}$
Drawn wires	1720	1940	1.9
Stabilized wires	1615	1850	5.1

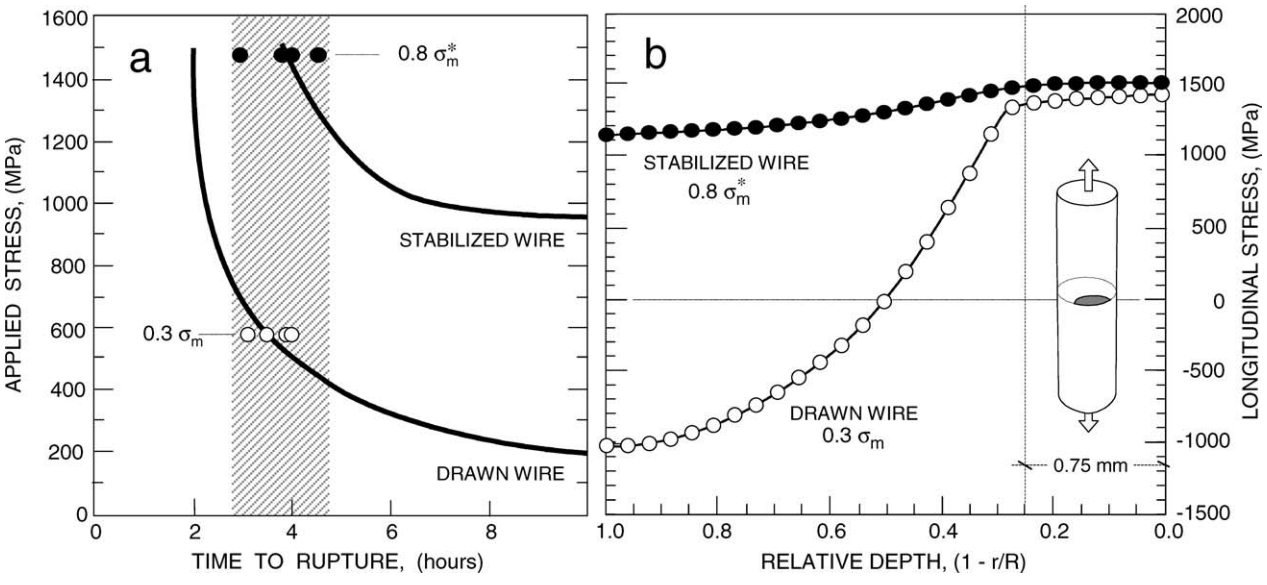

Figure 11 Wires with different profiles of residual stresses may show similar times to fracture when tested at quite different loads: (a) Hydrogen embrittlement test. Rupture times for eutectoid cold drawn wires and stabilized ones. (b) Profiles of longitudinal stresses in drawn ($\sigma_m = 1940$ MPa) and stabilized wires ($\sigma^*_m = 1850$ MPa) when the wire is stressed at different loads.

longitudinal residual stresses may give a cue to this behaviour, if we realize (see Fig. 11) that in both cases, the skin of the wire is supporting a similar stress field.

6. Final comments and conclusions

Eutectoid steel, when properly drawn, furnishes wires of exceptional quality and performance. They are indispensable in prestressed concrete structures, where stress relaxation losses have to be limited, in suspension bridges or in cables in mine shafts, where environment assisted cracking has to be avoided, or in tyre reinforcements, where fatigue is of concern. In all these circumstances, the mechanical performance of the cold-drawn wires depends on its microstructure and the presence of defects —inclusions or surface defects—. The role of residual stresses in the mechanical behaviour was suspected from the very beginning, but the lack of suitable tools for measurement and prediction of residual stresses kept this question in abeyance. The advent of powerful computers and the availability of equipment to perform diffraction measurements, with neutron and X-ray sources, has allowed accurate measurements and simulations of the residual stress profiles.

This paper shows how *stress relaxation losses* are influenced by residual stresses whose values add to the external loads and modify the viscoplastic response of the wire. The influence of pre-stretching loads, or of stress relieving treatments, on stress relaxation losses can be understood when the profile of residual stresses is known. The worrying problem of *environmental assisted cracking* is related, in some cases, to the presence of tensile surface residual stresses; some awkward results in times to fracture during hydrogen embrittlement tests can be explained if accurate values of residual stresses, near the wire surface, are known. *Fatigue life* is also influenced by residual stresses as well as fracture by *delamination*, a topic not discussed here [37]. The shape of the stress-strain curve during a *tensile test* is also related to the presence of residual stresses, to the extent that by comparison of the tensile curves of different wires it is possible to infer the presence of residual stresses in some of them. No doubt, the awareness of the role of residual stresses in the performance of cold-drawn wires will gain ground with the improvements of computing power and measurement techniques.

Acknowledgements

The author is very grateful for the help of Prof. J.M. Atienza in performing numerical simulations and testing, to Prof. J. Ruiz for measurements with X-ray and hydrogen embrittlement tests, to Prof. F.J. Mompeán and collaborators for neutron diffraction measurements and to Prof. G.V. Guinea for helpful discussions. The author gratefully acknowledges the support of the Spanish Ministry of Science and Technology grants MAT01.3863.C3 and MAT 2000-1334.

References

1. T. TARUI, T. TAKAHASHI, H. TASHIRO and S. NISHIDA, in "Metallurgy, Processing and Applications of Metal Wires," edited by H. G. Paris and D. K. Kim (The Minerals, Metals & Materials Society, 1996).
2. J. M. GARCIA-MONAR, (private communication).
3. A. B. DOVE, in "Ferrous Wire" (The Wire Association International Inc., 1989) Chap. 1.
4. J. D. EMBURY and R. M. FISHER, *Acta Metall.* **14** (1966) 147; E. M. TALEFF, C. K. SYN, D. R. LESUER and O. D. SHERBY, *Metall. Mater. Trans.* A **27** (1996) 111.
5. E. M. TALEFF, J. J. LEWANDOWSKI and B. POURLADIAN, *JOM*, July (2002) 25.
6. N. J. GIMSING, "Cable Supported Bridges" (John Wiley & Sons, 1997).
7. T. TAKAHASHI, I. OCHIAI and H. SATOH, Nippon Steel Tech. Report N53, 1992.
8. M. ELICES, *Informes de la Construcción* **396** (1988) 5. (In Spanish).
9. *Idem.*, in "Fracture Mechanics of Concrete," edited by G. C. Sih and A. DiTommaso (Martinus Nijhoff Publ., 1985) Chap. 5.
10. B. POURLADIAN and D. HARE, *Wire J. Intern.* July (2002) 77.

11. K. F. MCGUINN and M. ELICES, *Brit. Corros. J.* **16** (1981) 187.
12. M. A. ASTIZ, A. VALIENTE, M. ELICES and H. D. BUI, in "Life Assessment of Dynamically Loaded Materials and Structures" edited by L. Faria (1984) Vol. 1, p. 385.
13. O. C. ZIENKIEWICZ and R. L. TAYLOR, "The Finite Element Method" (McGraw-Hill, Inc., 1989).
14. HIBBITT, KARLSSON and SORENSEN, "ABAQUS User's Manual, Version 5.8," 1988.
15. A. J. L. CROOK and E. HINTON, in Proceedings 1st. Int. Conf. on Computational Plasticity, Barcelona (Pineridge Press Ltd., 1987) p. 181.
16. K. J. BATHE, M. KOJIC and J. WALCZAK, in Proceedings 2nd. Int. Conf. on Computational Plasticity, Barcelona (Pineridge Press Ltd., 1989) p. 263.
17. T. HAMADA, T. HIROUCHI and M. AKIYAMA, *Wire J. Intern.* May (2001) 86.
18. J. M. ATIENZA, "Residual stresses in drawn steel wires," Ph.D. Thesis. Universidad Politécnica de Madrid, 2001.
19. E. MACHERAUCH and K. H. KLOOS, in Proceedings Int. Conf. on Residual Stresses, Garmish 1986 (Oberursel 1987) p. 3; P. VAN HOUTTE and L. DE BUYSER, *Acta Metall. Mater.* **41** (1993) 323.
20. J. M. ATIENZA and M. ELICES, *Mater. Struct.* **37** (2004).
21. J. M. ATIENZA, M. MARTINEZ, F. J. MOMPEAN, M. GARCIA-HERNANDEZ, J. RUIZ and M. ELICES, in Proceedings 14th European Conference on Fracture, edited by A. Neimitz *et al.* (EMAS Pub., 2002) p. 113.
22. K. VAN ACKER, J. ROOT, P. VAN HOUTTE and E. AERNOUDT, *Acta Mater.* **44** (1996) 4039; J. RUIZ, J. M. ATIENZA and M. ELICES, *J. Mater. Engng. Perform.* **12** (2003) 480.
23. Model Code CEB-FIP (1990). ASTM-A421 (1991). BS-2691 (1991).
24. J. R. LIBBY, "Modern Prestressed Concrete" (van Nostrand Reinhold Co., 1977).
25. J. M. ATIENZA and M. ELICES, *Mater. Struct.* **36** (2003) 262.
26. ASTM E328-86 Standard Test Methods for Stress Relaxation Tests for Materials and Structures (1996).
27. J. M. ATIENZA (private communication).
28. S. SURESH, "Fatigue of Materials" (Cambridge U.P., 1998).
29. J. LLORCA and V. SANCHEZ-GALVEZ, in "Computational Plasticity," edited by D. R. J. Owen, E. Hinton and E. Oñate (Pineridge Publ., 1987) p. 1123.
30. *Idem.*, *Fatigue Fract Engng. Struct.* **12** (1989) 31.
31. K. KATAGIRI, T. SATO, K. KASABA, S. SASAKI and H. TASHIRO, *ibid.* **22** (1999) 753.
32. D. G. ENOS and J. R. SCULLY, *Metall. Mater. Trans.* A **33** (2002) 1151.
33. FIP-78, "Stress Corrosion Test", Technical Report 5 (Wexham Springs, 1978).
34. M. ELICES, G. MAEDER and V. SANCHEZ-GALVEZ, *Brit. Corr. J.* **18** (1983) 80.
35. V. SANCHEZ-GALVEZ and M. ELICES, in "Life Assessment of Dynamically Loaded Materials and Structures," edited by L. Faria, (1984), p. 1003.
36. M. ELICES, J. RUIZ and J. M. ATIENZA, *Mater. Struct.* **37** (2004).
37. N. IBARAKI, K. MAKII, K. OCHIAI and Y. OKI, *Wire J. Intern.* March (2000) 122.